DISTRIBUTION STATEMENT A. Approved for public release; distribution is unlimited.

Improving Estuarine Transport Models using Satellite Measurements

Stefan A. Talke
Civil and Environmental Engineering Department, Portland State University
PO Box 751-CEE
Portland, OR 97207-0751
phone: (503) 725-2870 fax: (530) 725-4282 email: talke@pdx.edu

Award Number: N00014-13-1-0084

LONG-TERM GOALS

Satellite measurements continue to improve and now provide an opportunity to interpret estuary processes over an unprecedented range of spatial scales. Because surface images of water level, water temperature, salinity, and turbidity are surface manifestations of underlying physical processes, they can be used to obtain information about tidal processes, river flow, and bathymetry. Improved understanding of remotely-sensed surface patterns provides a means for testing and improving numerical models, particularly in areas in which limited or no measurements are available.

OBJECTIVES

The overall objective of the project "Improving Estuarine Transport Models using Satellite Measurements" is to investigate the spatial variability of surface sediment concentrations, salinity, and water temperature in estuaries, thereby improving knowledge of processes and providing constraints for models. The specific objective is to address the following questions:

- *What insights into sediment distribution, salinity, and water temperature in estuaries can be gained by collating and mining satellite images from 15+ years of MODIS satellite measurements and higher resolution LANDSAT images?*
- *Can canonical relationships for the longitudinal distribution of scalars such as salinity and turbidity be observed in satellite data under different physical conditions?*
- *Can satellite measurements of water level and scalars be used to determine system response and calibrate numerical models as a function of river flow and tidal forcing?*

APPROACH

A three-fold approach has been used since the project started in Dec. 2012. First, we are developing and refining our processing of satellite measurements, using the Columbia River estuary (CRE; Fig. 1) as a test case due to the availability of in-situ measurements and local knowledge. Second, we are actively developing analytical and numerical modeling capabilities for stratified conditions which we are using to improve process knowledge and interpret results from satellite measurements. Finally, we are exploring how to estimate tides and river slopes via remote sensing (Lidar). In past reports we have

focused on turbidity distribution; here, we also present new measurements of water temperature (T_w) and salinity, and discuss advances in our understanding of Lidar-based tide measurements.

***Satellite Processing**:* We estimate turbidity and water temperature by regressing in-situ measurements against appropriate bands of surface reflectance measured by two missions: (1) the MODerate Imaging Spectrometer (MODIS) installed on the Terra and Aqua satellites, with pixel sizes from 250 to 1000m and a return period of 1 day and (2) Landsat, with pixel sizes from 30 to 120m and a return period of 16 days. Level 2 satellite data with atmospheric corrections are obtained from http://ladsweb.nascom.nasa.gov/ and are used for turbidity estimation; Level 1 data is used to estimate T_w using Planck's black body radiation equation and an estimated emissivity for water of 0.985. Data are calibrated to and compared against in-situ data obtained from the CMOP network: http://www.stccmop.org/datamart/observation_network. All satellite data are filtered to remove data with clouds, aerosols, and poor quality, and a total of >1500 good MODIS images and 70 Landsat images since 1999 have been analyzed. Additional river flow, tidal, and wave data are obtained from USGS, NOAA CO-OPS, and NBDC. We are also working on interpreting water temperature and turbidity data from the Ems Estuary; this work is 'in progress' and will be discussed next year.

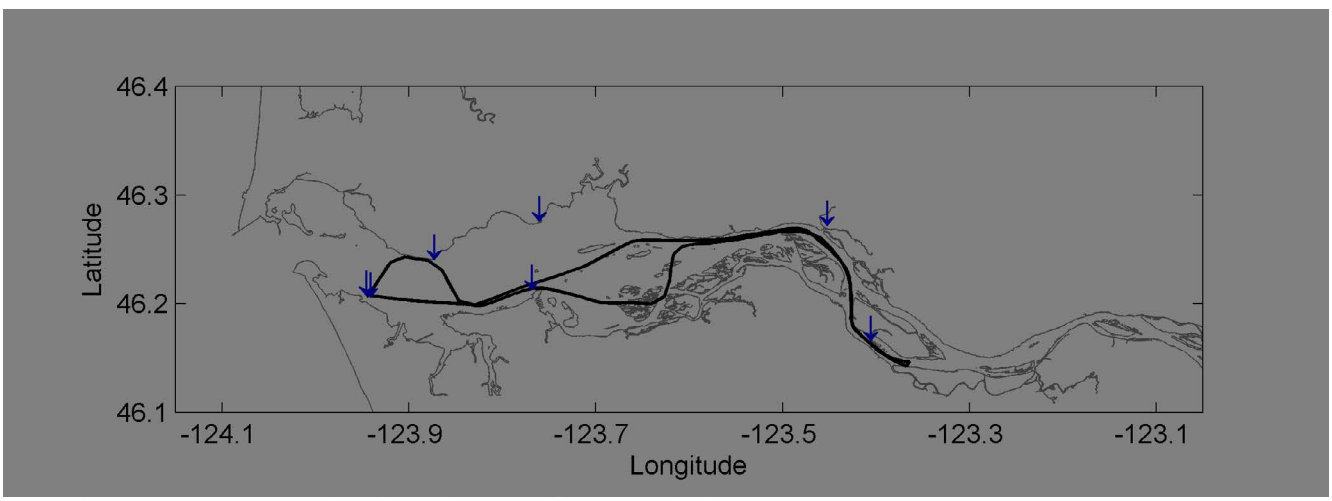

Figure 1: Transects flown during the June 2013 LIDAR experiment on the Columbia River Estuary. Locations of tide data shown with arrow.

***Modeling and Interpretation**:* One of the challenges in interpreting surface satellite data is that some estuaries—such as the CRE—are often stratified, such that surface conditions may not accurately represent bottom conditions. To better understand the physics of stratified systems, and how river flow, tidal forcing, and bathymetry interact together to produce a surface signal, we have developed semi-analytical models of both salinity and turbidity distribution. Our analytical approach modifies the MacCready (2007) salinity intrusion model to include the asymmetry in tidal mixing between flood and ebb (Jay& Musiak, 1994; Jay, 2010). Essentially, the along channel, tidally averaged circulation is modeled as a function of a constant density field (gravitational circulation, U_{GC}), the tidally varying density field (internal asymmetry, U_{IA}), and river flow (U_R). The derivation of U_{IA} is complex and involves using a perturbation expansion, a tidally varying eddy viscosity, and an iterative procedure to solve for the tidal (time varying) velocity and density field (details in Hudson, 2014). Nonetheless, the vertical structure of U_{IA} is similar to the well-known U_{GC}, with near bed circulation directed

upstream and a return flow evident in the upper water column (Fig. 2). For most conditions, U_{IA} is larger, as shown in the following scaling:

$$U_{GC} \propto \left(\frac{\Delta\rho_H g H^2}{L_s \rho_o u_*}\right); \qquad U_{IA} \propto \frac{U_o}{\omega L_s}\left(\frac{\Delta\rho_H g H^2}{L_s \rho_o u_*}\right).$$

Circulation increases nonlinearly with depth H, is proportional to the horizontal density gradient $\Delta\rho/L_s$, and inversely proportional to mixing (friction velocity u_*). Compared to U_{GC}, circulation due to U_{IA} is even more sensitive to the length of the salinity gradient (thru L_s), but also depends on tide wave frequency ω. We hypothesize that spring-neap changes in tidal velocity U_o, tidal damping due to river flow, and annual tidal variability will feedback into the salinity and turbidity distribution.

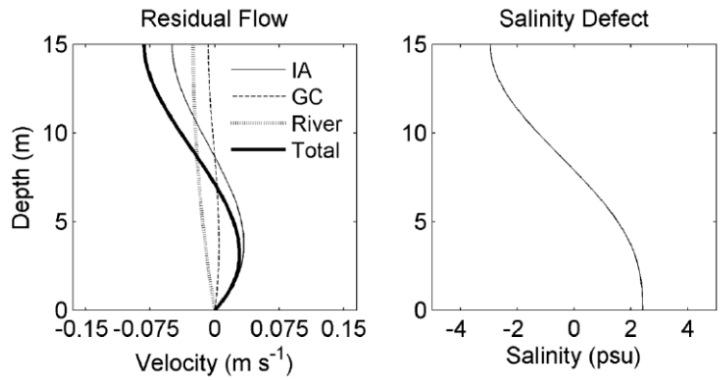

Figure 2: Comparison of salinity anomaly and tidally-averaged circulation from internal asymmetry, gravitational circulation, and river flow in an idealized, semi-analytical model (Hudson, 2014).

The approach outlined above is used to solve for the along-channel density structure by solving the salinity mass balance equation (an iterative solution technique is used-see Hudson 2014). The circulation is used as input into a semi-analytical sediment transport model, following the 'morphodynamic equilibrium' approach outlined by Talke et al., 2009 (see also Hudson, 2014). These models suggest that many useful parameters can be estimated via remote sensing, such as the length of the salinity gradient (L_s) .and the horizontal density difference $\Delta\rho_H$ (function of both salinity and temperature), the position of the ETM, the distribution of turbidity, and the position of salinity intrusion, which is proportional to Q^{-n} (n can vary between ≈1/7 and 1).

Lidar-based Tide measurements: A final way in which remote sensing may help interpret estuary functioning is through direct estimation of the tidally averaged river slope and tidal amplitudes. In June 2013, surface temperature imagery and Lidar elevation data were collected from Rkm 15 to 75 (Fig. 1) using the APL (Applied Physics Laboratory) airborne remote sensing system. Multiple transects (8 total) were run, allowing up to 16 repeat measurements of the same location over a 16 hour period. Corrections for plane elevation, pitch, and roll are made via GPS, and data over land or when the plane was banking are filtered out. A curve containing an M2 tide is fit to data every km. Absolute heights are estimated using the EGM 2012 Geoid, and both mean water level and tidal variability are compared against in-situ data at 7 locations.

WORK COMPLETED

Over the past year we have improved our calibration of satellite data to include high resolution Landsat images of the CRE and other estuaries, and have explored methods of estimating salinity from the resulting images. Error analysis has been added to our analysis of turbidity profiles, and improved interpretation of results has been incorporated into a Master's thesis (Hudson, 2014) and a journal manuscript (Hudson & Talke, 2015, submitted). The theory behind estuary turbidity maxima (ETM) and methods of assessing ETM using remote sensing were incorporated into a review paper that was recently accepted (Jay, Talke, et.al 2015). Improvements have been made in processing of Lidar measurements, in particular related to the assessment of the mean river slope. A manuscript describing LIDAR based tide measurements is expected to be submitted in the next month. Two conference presentations have been made over the past year, and four more are planned by Mar. 2016.

RESULTS

Regressions of Landsat reflectance to *in-situ* water temperature exhibit excellent correlation values and an rms error of ~1 degree Celsius when high-quality, low-aerosol data are used (R^2>0.9). This calibration yields high resolution snapshots (60-120m) which depict the variability of Tw over the estuary (Fig. 3). Analysis of multiple figures (not shown) suggests that the pattern observed in the Tw map—that is, cool ocean water intruding along the north side of the estuary, and warmer river water flowing down the south side of the estuary—is a typical pattern and occurs because the shipping channel on the south side carries most of the river flow.

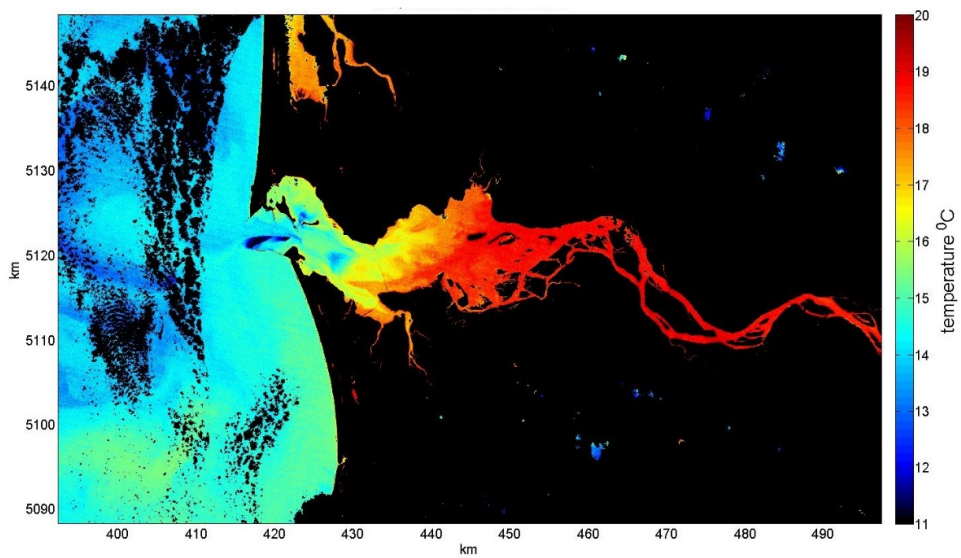

Figure 3: CRE water temperature from a Landsat image on 9/6/2002. Note offshore clouds.

To convert water temperature to salinity we use two strategies. First, for time periods with sufficient in-situ data, a direct estimate of salinity is possible using a T-S diagram (see e.g. Palacios et al., 2009). This approach works especially well when the contrast between river and ocean Tw is large in summer (Fig. 4a). However, since the T-S relationship continually changes, both due to daily heating and seasonal time scales, another approach is needed for time periods with no in-situ data. Hence, we have explored regressing salinity against normalized water temperature, defined as $T_* = \frac{|T_{meas} - T_{River}|}{|T_{Ocean} - T_{River}|}$

.

Results (Figure 4b) suggest that, on a seasonal basis at least, results can be collapsed and a first order estiamate of salinity can be made on the basis of only water temperature measured by Landsat. However, while the river Tw is reasonably estimated to within 1 degree rms Celsius by the Landsat measurement, results show that the ocean water boundary condition is more problematic. In Figure 5, we find a decent representation of surface salinity obtained only through analysis of T_w in Fig 3. However, close observation suggests we are under-estimating the salinity at the ocean, probably since most surface water is warmer than our selected value. Implicitly, this result indicates that the ocean near the estuary mouth is variable and possibly stratified. In-situ data suggests that cooler, deeper ocean water is entering the estuary than is measured at the surface. We are investigating whether other Landsat bands (which represent scalars such as turbidity) could improve salinity estimates.

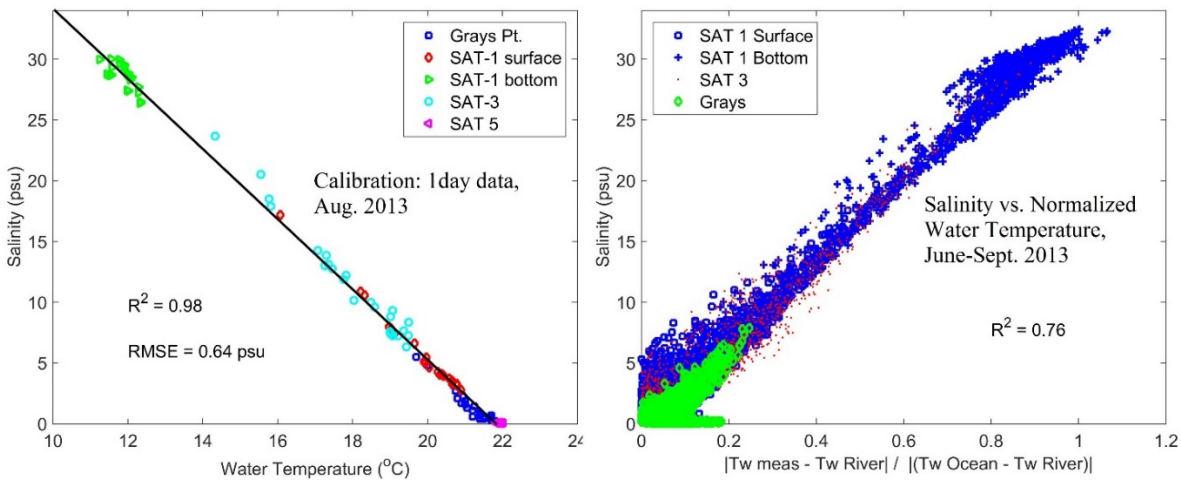

Figure 4: T-S diagrams in the CRE

The patterns of water temperature and salinity observed in Figure 3 and 5 are interesting to compare against improved estimates of the along-channel turbidity distribution (Fig. 6). During low flow or neap conditions, the turbidity maximum in both the south channel and the north channel moves upstream; during spring tides and high flow conditions, the ETM moves downstream. The south channel salinity intrusion appears to be well correlated with the ETM position, although a persistent increase in turbidity is observed at Rkm 15 in most conditions except neap tides. The north channel proves interesting; while Fig. 5 suggests that the north channel is more saline at the surface, the ETM actually appears to be further downstream (closer to the inlet) for most conditions. This is most likely due to trapping of turbidity (in both channels) due to a series of topographic holes.

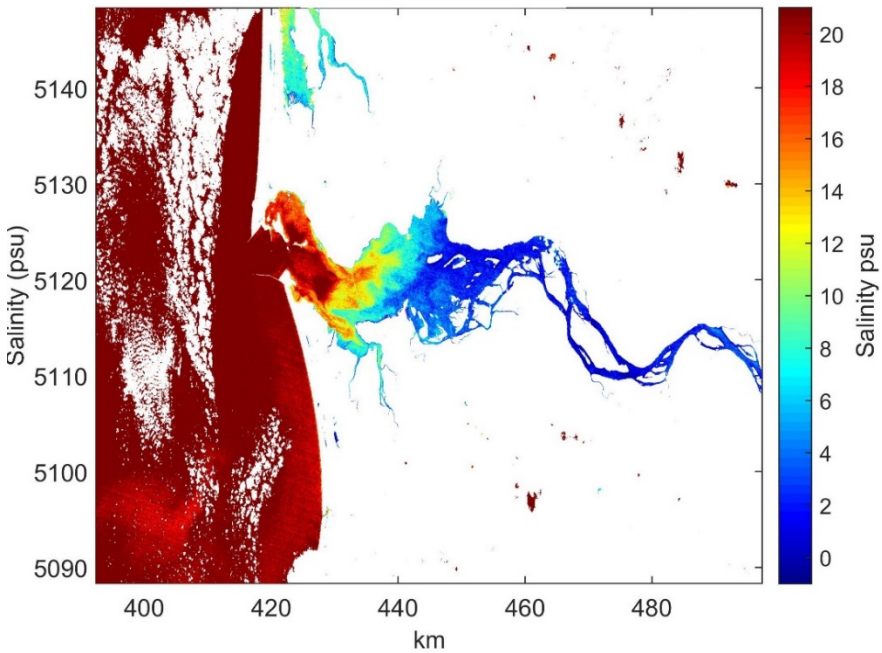

Figure 5: Salinity estimate using Landsat and normalized Temperature calibration for Sept. 6, 2002

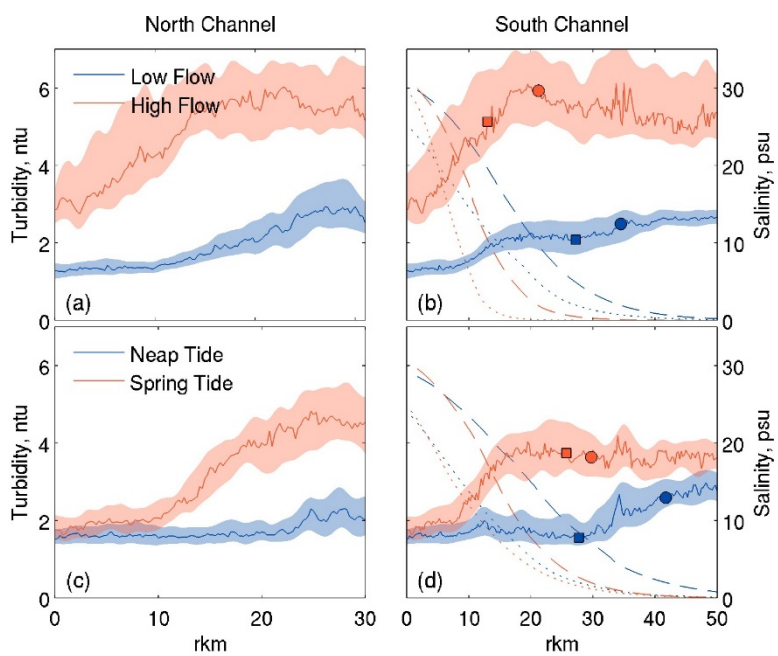

Figure 6: Turbidity distribution based on Modis comparing spring-neap conditions (average flow) and high/low flow (average tidal conditions) in both the North and South Channels. Dotted lines is estimated salinity structure.

We investigate the processes leading to the turbidity distribution by running model experiments with realistic (but smooth) topography (Fig 7) and a number of idealized studies. Fig. 7 shows how the

ETM position X_{max} moves downstream as river flow and tidal amplitude increase. In a flat, constant depth model (H =15m), X_{max} varies smoothly as joint function of river flow and tidal amplitude (Case I, Fig 8a). A topographic sill (Case II, Fig 8b) tends to crowd the ETM downstream of the sill; the number of river flow/tidal flow combinations that produces an ETM between Rkm 10 and 20 has increased relative to Fig. 7a. For a topographic low, the situation is reversed, and a larger parameter space produces an ETM between Rkm 20 and 40. All these features are evident in a topographically complex situation(Case IV, Fig. 8d). Perhaps paradoxicially, the complexity results in a more stable ETM zone which doesn't migrate as far downstream or upstream.

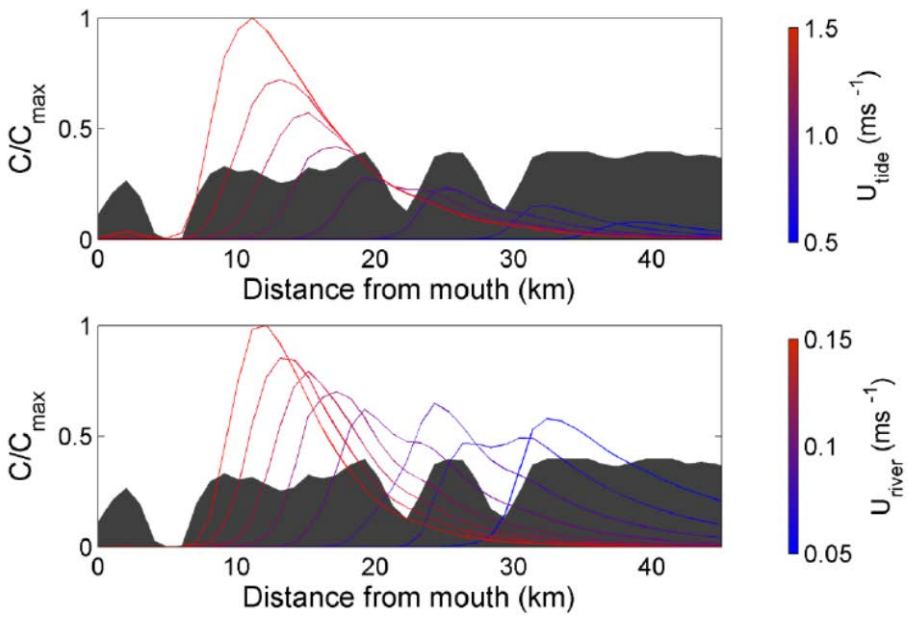

Figure 7: Turbidity distribution from idealized model using variable topography and different flow/tidal forcing. Qualitatively, the observed patterns from Fig. 6 are reproduced.

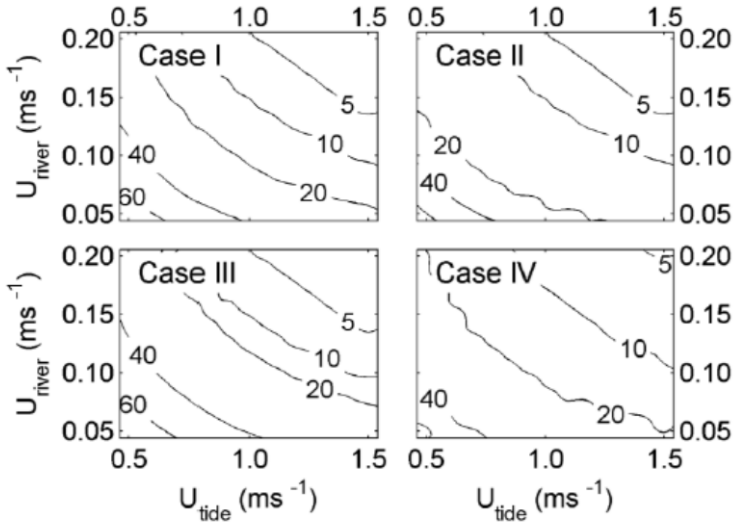

Figure 8: Position of the ETM maximum (contours in Rkm) as a function of river flow and tidal velocity for Case I (constant depth), Case II (5 m sill at Rkm 20), Case III (5m hole at Rkm 20) and Case IV (topography as in Figure 7; approximates CRE).

The turbidity features observed in Figs. 6 thru 8 assume that channel processes—rather than waves—dominate the turbidity distribution. Initial correlation analysis suggested this assumption held (Hudson, 2014); however, an improved correlation that considers only the east/west component of wind, median flow conditions, and wind speed above a threshold (2 m/s) yields statistically significant correlation in shallow parts of the CRE. The correlation hot spots point to the existence of turbidity maxima produced by wind waves and ocean swell, though increased reflectance due to wave breaking may be a factor. Interestingly, a seasonal difference is observed; summer winds are predominately eastward, while winter winds often reverse direction. Such analysis can be used to outline locations of subtidal habitat.

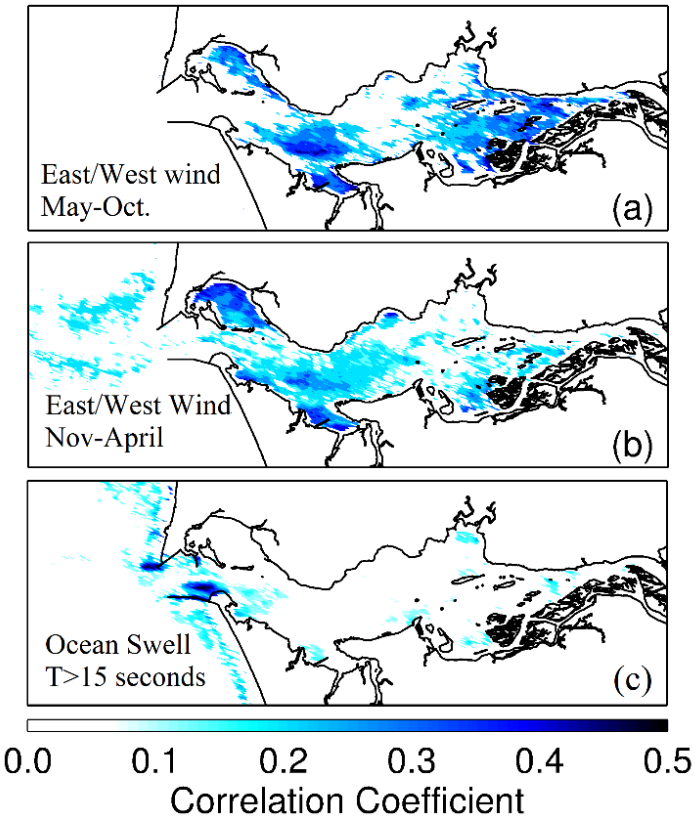

Figure 9: Correlation of MODIS Band 2 reflectance against the east/west component of wind and offshore ocean swell. Areas of high correlation (>0.3) are generally shallow subtidal.

Lidar Tides: The Lidar Tides experiment demonstrates that tides and water level slope can be approximated via airborne remote sensing (Fig. 10, 11). Several issues prevent ideal comparison of tidal amplitudes and river slope. First, the datum error in the CRE can be 10-20 cm (NOAA V-datum), such that even the river slope between tide gauges is not exactly known. Second, the geoid solution in the CRE are still being refined and large variations in predicted slope occur between different generations of the EGM geoid. The best comparison to in-situ data was found with the most modern, EGM 2012 geoid and yielded slopes that agreed to within 50% (Fig. 11). More transects would likely reduce error, especially for Rkm > 50. Finally, the Lidar and GPS were not well synched in time, and error levels were larger than the factory-suggested rms error of 0.1m. Still, the experiment demonstrates 'proof-of-concept' and suggests that improvements in the geoid and in experimental execution can make the method viable.

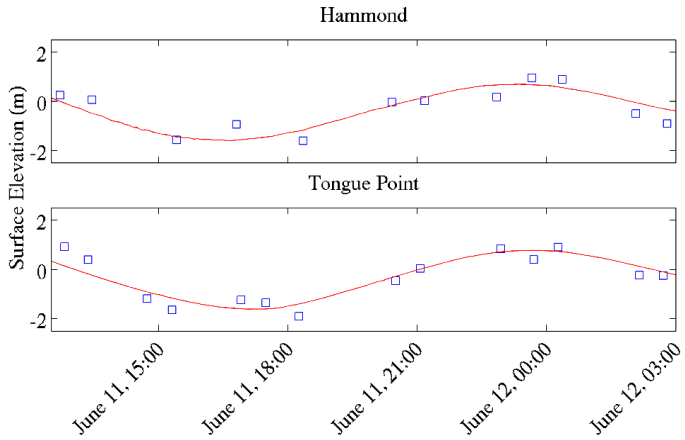

Figure 10: Comparison of tides measured using airborne Lidar (blue) with tide gauges (red)

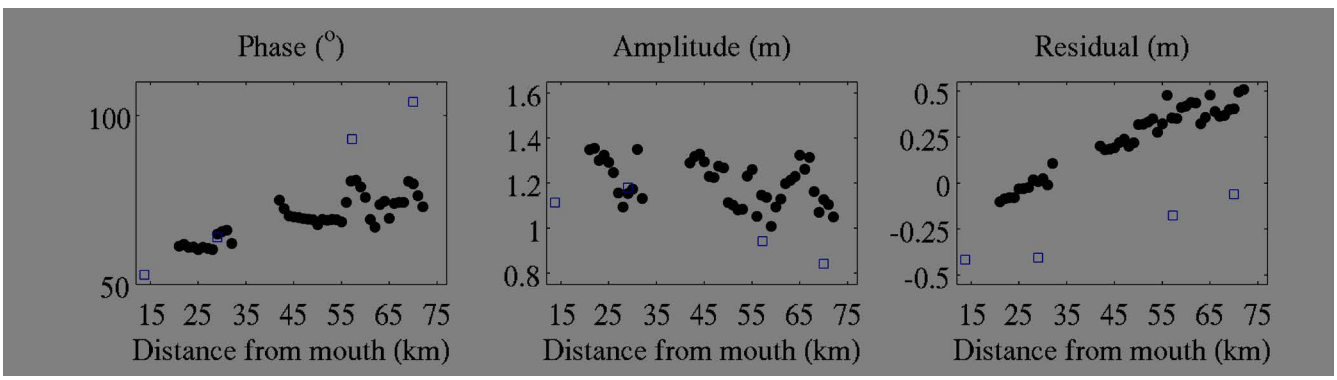

Figure 11: Comparison of in-situ gauge results (blue) against Lidar results (black)

IMPACT/APPLICATIONS

Our study aims to use the full satellite record to define statistically representative states that vary over the full range of forcing. The resulting analysis can be used to help locate bathymetric features, calibrate the distribution of salinity and turbidity in numerical models, and characterize spatio-temporal variability that is not possible with *in-situ* monitoring. The 'big data' approach enables monitoring of locations with limited data and gets around the poor temporal resolution of satellite data. Analytical modeling helps define important parameters that can be monitored remotely.

Using Lidar to estimate tides is a simple way to remotely estimate tides and river slope in areas in which insufficient data is available. Since water level data is a fundamental necessity for numerical models, remotely measuring tides could be used to help initialize and calibrate hydrodynamic and transport models in hard-to-measure areas such as shallow channels and tidal flats. Further, tides contain more information than just water level: the rate of spatial damping is related to friction and river flow, while the tidal propagation speed is a function of depth, friction, and convergence. These known relationships can be inverted to estimate friction and depth.

RELATED PROJECTS

The recent NSF-sponsored Career award, "Modeling 19th-century estuaries to address 21st-century problems" provides funds to simulate water temperatures in the Columbia River Estuary using Delft3D; this will help with interpreting and analyzing spatial patterns of water temperature and salinity in Landsat images. A recently funded project by Tierra Solutions (a private company) will apply the methods developed in this grant to high-resolution, private-party satellite data (1m resolution) in the polluted Passaic River estuary.

REFERENCES

Hudson, A., 2014. Applications of Remote Sensing to the Study of Estuarine Physics: Suspended Sediment Dynamics in the Columbia River Estuary. *Masters Thesis,* Portland State University (Advisor: S.A. Talke).

Jay, David A., Jeffery D. Musiak. (1994). Particle Trapping in estuarine tidal flows. *Journal of Geophysical Research,* 99 p. 20,445-20,461.

Jay, David A. (2010). Estuarine Variability. *Contemporary Issues in Estuarine Physics.* 1 p. 62-99.

Jay, D.A., S.A. Talke, A. Hudson, 2015 *in press*. Estuarine Turbidity Dynamics Revisited: Instrumental approaches, remote sensing, modeling studies, and new directions. *Chapter 3 in book on Sediment dynamics,* J. Best (editor)

MacCready, Parker. (2007). Estuarine Adjustment. *Journal of Physical Oceanography*, 37 p. 2133-2145. doi: 10.1175/JPO3082.1

Palacios, L. Sherry. Tawnya D. Peterson., Raphael M. Kudela. (2009). Development of synthetic salinity from remote sensing for the Columbia River Plume. *Journal of Geophysical Research*, 114C00B05. doi:10.1029/2008JC004895.

Talke, S.A, H.E. De Swart & H.M.Schuttelaars, 2009. Feedback between residual circulation and sediment distribution in highly turbid estuaries: an analytical model. *Continental Shelf Research*, 29(1) p. 119-135. doi:10.1016/j.csr.2007.09.002

HONORS/AWARDS/PRIZES

CAREER Award, National Science Foundation, 2015-2020 (Talke)